

**Steven Johnson,^{a,b} Pietro
 Roversi,^a Mariana Espina,^c
 Janet E. Deane,^a Susan Birket,^c
 William D. Picking,^c Ariel
 Blocker,^b Wendy L. Picking^c and
 Susan M. Lea^{a,b,*}**

^aLaboratory of Molecular Biophysics,
 Department of Biochemistry, University of
 Oxford, England, ^bSir William Dunn School of
 Pathology, University of Oxford, England, and
^cDepartment of Molecular Biosciences,
 University of Kansas, USA

Correspondence e-mail:
 susan.lea@path.ox.ac.uk

Received 3 May 2006
 Accepted 12 July 2006

Expression, limited proteolysis and preliminary crystallographic analysis of IpaD, a component of the *Shigella flexneri* type III secretion system

IpaD, the putative needle-tip protein of the *Shigella flexneri* type III secretion system, has been overexpressed and purified. Crystals were grown of the native protein in space group $P2_12_12_1$, with unit-cell parameters $a = 55.9$, $b = 100.7$, $c = 112.0$ Å, and data were collected to 2.9 Å resolution. Analysis of the native Patterson map revealed a peak at 50% of the origin on the Harker section $\nu = 0.5$, suggesting twofold non-crystallographic symmetry parallel to the b crystallographic axis. As attempts to derivatize or grow selenomethionine-labelled protein crystals failed, in-drop proteolysis was used to produce new crystal forms. A trace amount of subtilisin Carlsberg was added to IpaD before sparse-matrix screening, resulting in the production of several new crystal forms. This approach produced SeMet-labelled crystals and diffraction data were collected to 3.2 Å resolution. The SeMet crystals belong to space group $C2$, with unit-cell parameters $a = 139.4$, $b = 45.0$, $c = 99.5$ Å, $\beta = 107.9^\circ$. An anomalous difference Patterson map revealed peaks on the Harker section $\nu = 0$, while the self-rotation function indicates the presence of a twofold noncrystallographic symmetry axis, which is consistent with two molecules per asymmetric unit.

1. Introduction

Shigella flexneri, the causative agent of shigellosis, is a Gram-negative bacterial pathogen that initiates infection by invading cells of the colonic epithelium in a process which is dependent on a type III secretion system (T3SS; Phalipon & Sansonetti, 2003). The T3SS is composed of a basal body, which traverses both bacterial membranes, and an external needle through which effector proteins are secreted (Blocker *et al.*, 2001). During *S. flexneri* infection, secretion is activated by contact of the tip of the needle complex with host cells, resulting in formation of a pore in the host-cell membrane that is contiguous with the needle. Other effector proteins are injected *via* this apparatus directly into the host-cell cytoplasm (for a review, see Johnson *et al.*, 2005).

Of the T3SS effectors, IpaB, IpaC and IpaD are essential for invasion (Menard *et al.*, 1993). IpaB and IpaC have been demonstrated to insert into the host-cell membrane and are therefore suggested to form the translocation pore (Blocker *et al.*, 1999). Cells lacking IpaD are not only incapable of pore insertion and invasion, but also demonstrate impaired effector secretion control (Picking *et al.*, 2005). IpaD was originally proposed to form a plug in the T3SS with IpaB (Menard *et al.*, 1994), but more recent data has demonstrated that its role is more complex (Picking *et al.*, 2005). Deletions within the N-terminal third of the molecule do not affect invasion of the bacteria into host cells, although the insertion of IpaB/IpaC into membranes is slightly impaired. However, even short deletions (five residues) in the C-terminus of IpaD completely abolish the invasive phenotype and pore insertion. These observations, combined with the functional homology between IpaD and LcrV, a protein recently shown to be assembled at the tip of the *Yersinia pestis* T3SS needle (Mueller *et al.*, 2005), suggest that IpaD may play a role in regulating insertion of the IpaB/IpaC translocon pore from the tip of the *S. flexneri* needle.

Our laboratory has recently determined the crystal structure of MxiH, the needle subunit, and assembled a molecular model of the



© 2006 International Union of Crystallography
 All rights reserved

T3SS needle by docking it into a 16 Å EM reconstruction of the *S. flexneri* needle (Cordes *et al.*, 2003; Deane, Cordes *et al.*, 2006; Deane, Roversi *et al.*, 2006). As part of an ongoing study into the interactions of the T3SS with host cells, we have now expressed, purified and crystallized IpaD. The three-dimensional structure of IpaD, in conjunction with the structure of the MxiH needle and other tip proteins such as LcrV (Derewenda *et al.*, 2004), will hopefully allow us to delineate the mechanism of translocon insertion.

2. Experimental procedures

2.1. Expression and purification

The DNA fragment of the *ipaD* gene encoding residues 15–332 was produced using the methods described previously (Harrington *et al.*, 2003; Picking *et al.*, 2005) and subcloned into the pET-15b vector. This construct placed the gene in frame with an N-terminal hexahistidine tag. IpaD_{NΔ14} was expressed in *Escherichia coli* BL21 (DE3) cells grown in LB media containing 100 µg ml⁻¹ ampicillin. Cells were grown at 310 K to an *A*_{600 nm} of 0.6 and protein overexpression was induced by the addition of 1.0 mM IPTG. After 3 h, cells were

harvested by centrifugation (4000g, 15 min, 277 K) and pellets were frozen at 193 K. Cell pellets were resuspended in lysis buffer [20 mM Tris–HCl pH 7.5, 500 mM NaCl and Complete EDTA-free protease inhibitor cocktail (Roche)] and lysed using an Emulsiflex-C5 Homogeniser (Glen Creston, UK). The resultant cell suspension was centrifuged (20 000g, 30 min, 277 K) and the soluble fraction was applied onto a pre-charged 5 ml His-Trap HP nickel-affinity column (Amersham Biosciences). Protein was eluted using a gradient of 0–1 M imidazole in lysis buffer. Fractions containing IpaD_{NΔ14} were further purified by gel-filtration chromatography using a HiLoad 26/60 Superdex 75 column (Amersham Biosciences) equilibrated in 20 mM Tris–HCl pH 7.5, 100 mM NaCl, 10 mM DTT. IpaD_{NΔ14} eluted as a single monomeric peak and was demonstrated to be pure by SDS–PAGE; mass-spectrometric analysis (data not shown) confirmed the molecular weight of the protein minus the N-terminal methionine (37 374 Da). Fractions containing purified IpaD_{NΔ14} were pooled, concentrated using 5 kDa molecular-weight VivaSpin centrifugal concentrators (VivaScience, Sartorius Group) to approximately 70 mg ml⁻¹ and stored at 193 K in 50 µl aliquots.

SeMet-labelled IpaD_{NΔ14} was produced by expression in the *E. coli met⁻* auxotrophic strain B834 (DE3). Cultures were grown in LB media to an *A*_{600 nm} of 0.2, pelleted (4000g, 15 min, 277 K) and washed in phosphate-buffered saline three times. Washed cells were used to inoculate SelenoMet Medium Base containing SelenoMet Nutrient Mix, L-selenomethionine (40 µg ml⁻¹; Molecular Dimensions Ltd, UK) and ampicillin (100 µg ml⁻¹). Cultures were grown at 310 K until an *A*_{600 nm} of 0.6 was reached, whereupon the solutions were cooled to 293 K and protein overexpression was induced by the addition of 1.0 mM IPTG. After 16 h, cells were harvested and SeMet-labelled protein was purified as described above. Mass-spectrometric analysis confirmed full incorporation of SeMet, including the N-terminal methionine (data not shown), in contrast to the native protein. We assume this is a consequence of the incorporation of the selenium making the N-terminal peptide bond less likely to be cleaved.

2.2. Crystallization and limited proteolysis

Initial crystallization conditions were obtained by sparse-matrix screening (Jancarik & Kim, 1991) using the sitting-drop vapour-diffusion technique. Drops were prepared by mixing 0.2 µl protein solution (70 mg ml⁻¹, 20 mM Tris–HCl pH 7.5, 100 mM NaCl, 10 mM DTT) with 0.2 µl reservoir solution using a Tecan crystallization robot (Tecan UK, Theale, UK) and were equilibrated against 100 µl reservoir solution at 293 K. Initial crystals of IpaD_{NΔ14} (crystal form 1) grew in 3 d in condition No. 33 of Molecular Dimensions Screen 1 [30% (w/v) PEG 4000, 0.1 M Tris–HCl pH 8.5, 0.2 M MgCl₂]. Subsequent screening using handmade conditions yielded diffraction-quality crystals in PEG 4000 concentrations ranging from 25 to 28% (w/v). Mercury derivatives were prepared by adding 1 µl of 10 mM HgCl₂ in reservoir solution to the 0.4 µl drop. Crystals were soaked for 3 h at 293 K.

One IpaD_{NΔ14} crystal form (crystal form 2) grew over a period of 12 months in 10% (v/v) PEG 400, 0.1 M NaCl, 0.1 M Tris–HCl pH 7.0 (Fig. 1a) and was discovered to be an N-terminal truncation of IpaD_{NΔ14}. In an attempt to reproduce this and find new crystal forms, in-drop limited proteolysis was carried out (as in Gaur *et al.*, 2004). The broad-spectrum serine protease subtilisin Carlsberg from *Bacillus licheniformis* (Sigma–Aldrich) was added to IpaD_{NΔ14} in a 1:5000 enzyme:protein ratio by weight before sparse-matrix screening was carried out as described above. Diffraction-quality native crystals were obtained in Molecular Dimensions Screen 1 condition No. 24 [30% (v/v) PEG 400, 0.1 M Na HEPES pH 7.5, 0.2 M MgCl₂] (crystal

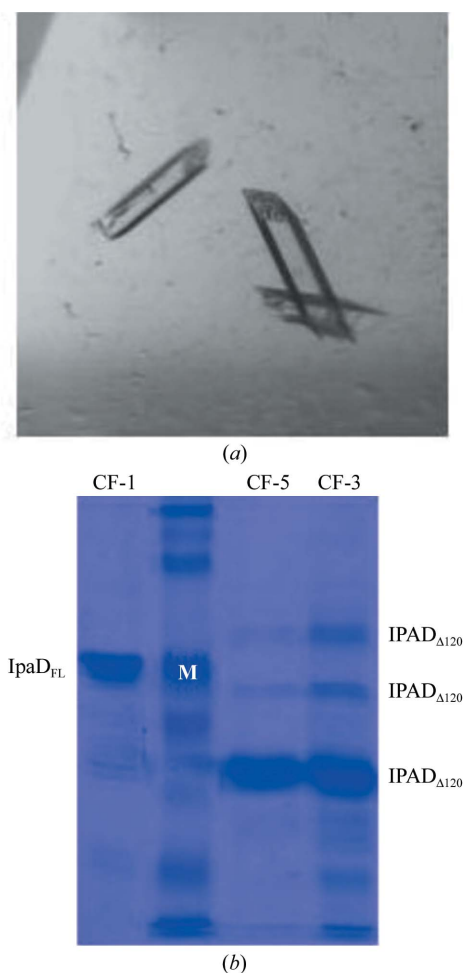


Figure 1
(a) Monoclinic crystals of IpaD crystal form 2 produced by in-drop proteolysis. (b) SDS–PAGE of protein derived from crystals with (CF-3 and CF-5) and without (CF-1) subtilisin treatment (see text for full description). The subscript denotes the portion of IpaD present in each band as determined by sequencing (FL, full length; Δ120, N-terminal deletion to residue 120). Molecular-weight markers are shown in lane 2; the marker identified with ‘M’ corresponds to a MW of 42 kDa.

Table 1
IpaD X-ray diffraction data-collection statistics.

Values in parentheses are for the highest resolution shells.

	CF-1		CF-2	CF-3	CF-4A	CF-4B SeMet MAD			CF-5	
	Native	Mercury soak	Native	Native	Native	Peak 1	Peak 2	Peak 3	Remote	Native
X-ray source	ESRF, ID14-3	ESRF, ID23-1	ESRF, ID14-1	ESRF, ID23-2	ESRF, ID23-1	ESRF, ID23-1			ESRF, BM16	
Detector	MAR CCD	MAR CCD	ADSC scanner	MAR CCD	ADSC scanner	ADSC scanner			MAR CCD	
Space group	$P2_12_12_1$	$P2_12_12_1$	$C2$	$C2$	$C2$	$C2$			$P2_1$	
Unit-cell parameters										
a (Å)	55.9	56.2	77.9	204.6	139.4	136.9			44.9	
b (Å)	100.7	102.4	91.5	45.1	45.0	44.3			205.9	
c (Å)	112.0	111.5	54.9	56.8	99.5	100.0			110.9	
β (°)			96.4	105.2	107.9	107.4			102.5	
Wavelength (Å)	0.931	1.0055	0.934	0.873	0.9757	0.9792	0.9792	0.9792	0.9757	0.9790
Resolution limits (Å)	75–2.7	38–3.2	42–2.0	30–3.5	43–2.8	34–3.4	34–3.4	34–3.2	48–3.3	41–3.9
	(2.8–2.7)	(3.4–3.2)	(2.1–2.0)	(3.7–3.5)	(3.0–2.8)	(3.6–3.4)	(3.6–3.4)	(3.4–3.2)	(3.5–3.3)	(4.1–3.9)
Completeness (%)	90.1 (68.2)	99.9 (100.0)	99.2 (99.8)	96.5 (96.5)	99.0 (96.3)	99.2 (96.4)	99.4 (96.7)	99.5 (100.0)	97.8 (87.5)	86.4 (86.7)
Unique reflections	14594	11143	24238	5840	14425	7938	8009	9703	8518	7495
Multiplicity	7.0 (3.0)	7.8 (7.9)	3.0 (3.0)	4.6 (4.7)	5.2 (4.6)	6.9 (6.6)	7.0 (6.8)	3.6 (3.7)	6.8 (6.2)	8.8 (8.2)
R_{merge}^\dagger	14.1 (48.2)	14.0 (37.2)	5.3 (41.8)	13.2 (41.6)	11.5 (29.2)	9.6 (33.6)	8.4 (23.1)	11.0 (33.5)	8.9 (25.8)	22.7 (42.1)
$I/\sigma(I)$	3.9 (1.6)	3.8 (1.8)	7.9 (1.7)	3.0 (1.5)	3.1 (1.9)	5.6 (2.2)	5.6 (3.0)	4.5 (2.0)	5.9 (2.7)	2.6 (1.7)
R_{anom}^\ddagger	—	—	—	—	—	6.7 (15.0)	5.5 (9.0)	5.4 (11.4)	4.0 (10.8)	—

$^\dagger R_{\text{merge}} = 100 \times \sum_h \left[\sum_i |I(h)_i - \langle I(h) \rangle| / \sum_i I(h)_i \right]$, where $I(h)_i$ is the i th observation of reflection h and $\langle I(h) \rangle$ is the mean intensity of all observations of h . $^\ddagger R_{\text{anom}} = 100 \times \sum_h |I^+(h) - I^-(h)| / \sum_h (I^+(h) + I^-(h))$, where $I^+(h)$ and $I^-(h)$ are the mean intensities of the Bijvoet pairs for observation h .

form 3) and Molecular Dimensions Screen 2 condition No. 19 [10% (w/v) PEG 8000, 0.1 M Na HEPES pH 7.5, 8% (v/v) ethylene glycol] (crystal form 4A; Fig. 1*b*). Diffraction-quality SeMet crystals were obtained in Molecular Dimensions Screen 1 condition No. 23 [28% (v/v) PEG 400, 0.1 M Na HEPES pH 7.5, 0.2 M CaCl₂] (crystal form 5) and Molecular Dimensions Screen 1 condition No. 34 [30% (v/v) PEG 400, 0.1 M Tris-HCl pH 8.5, 0.2 M sodium citrate] (crystal form 4B). Numerous other conditions in Molecular Dimensions Screens 1 and 2 yielded crystals that were too small to collect data from.

2.3. Data collection and processing

Crystal forms 1, 2, 3, 4A and 5 were cryoprotected in reservoir solution containing 20% (v/v) glycerol, 20% (v/v) PEG 400, 5% (v/v) PEG 400, 25% (v/v) ethylene glycol and 5% (v/v) PEG 400, respectively, and flash-cryocooled in liquid nitrogen prior to data collection. Crystal form 4B was mounted and flash-cryocooled directly in the cryostream.

Diffraction data were recorded at 100 K (Table 1). Data were indexed and integrated in *MOSFLM* (Leslie, 1992) and scaled with *SCALA* (Evans, 1997) within the *CCP4* program suite (Collaborative Computational Project, Number 4, 1994). A fluorescence scan on a

SeMet crystal (CF-4B) across the Se edge yielded values of $f' = -8.0$ and $f'' = 5.2$ using the program *CHOOCH* (Evans & Pettifer, 2001).

3. Results and discussion

Intact IpaD_{NΔ14} yielded plate-shaped crystals (CF-1) belonging to space group $P2_12_12_1$ (Table 1). Calculation of a native Patterson map revealed a peak at ~50% of the origin on Harker section $v = 0.5$, consistent with two molecules per asymmetric unit related by a pure translation (Fig. 2). The value of the Matthews coefficient is 2.1 Å³ Da⁻¹ for two molecules, corresponding to a solvent content of 42% (Matthews, 1968). Attempts to grow diffraction-quality SeMet crystals in this crystal form were unsuccessful. Soaking the crystals with mercury increased the quality of diffraction of the crystals but did not yield a reliable set of Hg sites, despite using the available Patterson-solving software.

During optimization of CF-1 a second crystal form was observed (CF-2) which took 12 months to grow and belongs to space group $C2$ (Fig. 1). One crystal was used for data collection and the remainder were re-solubilized, run on SDS-PAGE and N-terminal sequenced. This revealed a major band corresponding to an N-terminal truncation beginning at residue 144 (data not shown). The value of the Matthews coefficient is 2.4 Å³ Da⁻¹ for two molecules, corresponding to 49% solvent content.

The contents of CF-2 revealed that the N-terminal third of IpaD is susceptible to degradation and suggested that limited proteolysis could trim these regions. In an attempt to reproduce CF-2 and search for new crystal forms, the broad-spectrum protease subtilisin Carlsberg was added in trace amounts to IpaD_{NΔ14} before screening. Plate-shaped crystals were grown in three new crystal forms (CF-3, CF-4 and CF-5; Table 1) and analysis by SDS-PAGE revealed various degrees of N-terminal truncation (Fig. 1*b*). The value of the Matthews coefficient is 2.1 and 2.5 Å³ Da⁻¹ for CF-3 and CF-4, respectively, for two molecules per asymmetric unit and is 2.6 Å³ Da⁻¹ in CF-5 for four molecules.

Anomalous difference Patterson maps for SeMet derivatives of CF-4 were calculated within *autoSHARP* (Vonnrhein *et al.*, 2005) using $(E^2 - 1)$ coefficients and strict outlier rejection. The positions of ten Se atoms were obtained using the Patterson-solving software within

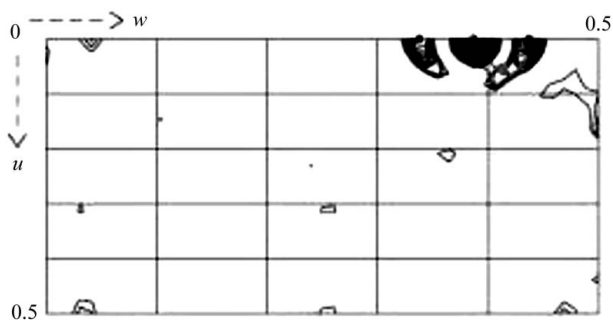


Figure 2
Harker section $v = 0.5$ of the native Patterson map of IpaD crystal form 1 calculated using *PATTERSON* (Collaborative Computational Project, Number 4, 1994) at 3.5 Å. The map is drawn with a minimum contour level of 1.5σ with 0.5 σ increments.

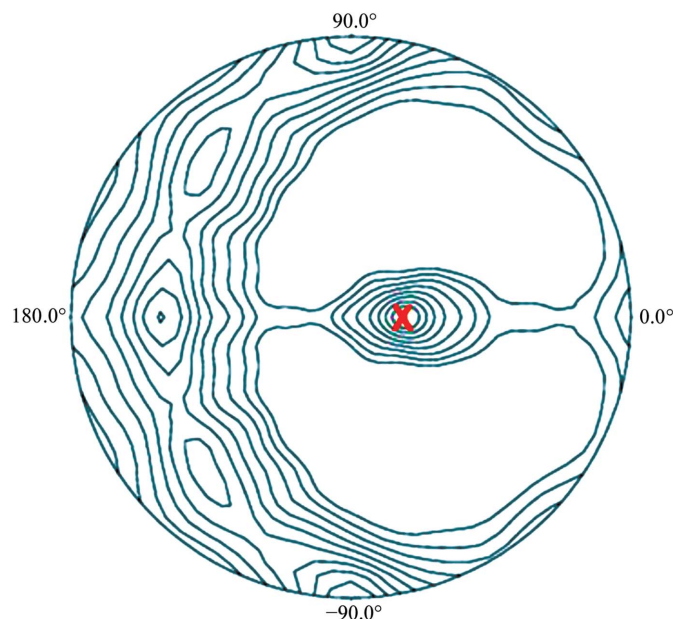


Figure 3
The $\kappa = 180^\circ$ section of the self-rotation function calculated for the crystal form 4 SeMet peak 1 data set using *MOLREP* (Collaborative Computational Project, Number 4, 1994) with an integration radius of 20.0 Å and data in the resolution range 15–4 Å. The peak (marked with an X) at $(\omega, \varphi) = (22, 0^\circ)$ represents 91% of the peak for the crystallographic twofold axis.

autoSHARP and were refined using *SHARP*. The ten sites clustered into two sets of five related by the twofold peak in the self-rotation function (Fig. 3). Structure determination and refinement in the various crystal forms is under way.

SJ is funded by a Medical Research Council of the UK grant (G0400389) to SML. PR is funded by a Wellcome Trust Grant (No. 077082) to SML and PR. JED is funded by an Australian National Health and Medical Research Council CJ Martin Postdoctoral Fellowship (ID-358785). WDP's laboratory was supported by PHS grants AI034428 and RR017708 and the University of Kansas

Research Development Fund. AB is funded by a Guy G. F. Newton Senior Research Fellowship. We are grateful to Ed Lowe for assistance with data collection and to Tony Willis for N-terminal sequencing. Marc Morgan and Jenny Gibson assisted with the crystallization robot and we are very grateful to Clemens Vornrhein for masterful processing of the orthorhombic native data.

References

Blocker, A., Gounon, P., Larquet, E., Niebuhr, K., Cabiaux, V., Parsot, C. & Sansonetti, P. (1999). *J. Cell Biol.* **147**, 683–693.
 Blocker, A., Jouihri, N., Larquet, E., Gounon, P., Ebel, F., Parsot, C., Sansonetti, P. & Allaoui, A. (2001). *Mol. Microbiol.* **39**, 652–663.
 Collaborative Computational Project, Number 4 (1994). *Acta Cryst.* **D50**, 760–763.
 Cordes, F. S., Komoriya, K., Larquet, E., Yang, S., Egelman, E. H., Blocker, A. & Lea, S. M. (2003). *J. Biol. Chem.* **278**, 17103–17107.
 Deane, J. E., Cordes, F. S., Roversi, P., Johnson, S., Kenjale, R., Picking, W. D., Picking, W. L., Lea, S. M. & Blocker, A. (2006). *Acta Cryst.* **F62**, 302–305.
 Deane, J. E., Roversi, P., Cordes, F. S., Johnson, S., Kenjale, R., Daniell, S., Booy, F., Picking, W. D., Picking, W. L., Blocker, A. J. & Lea, S. M. (2006). *Proc. Natl Acad. Sci. USA*, doi:10.1073/pnas.0602689103.
 Derewenda, U., Mateja, A., Devedjiev, Y., Rutzahn, K. M., Evdokimov, A. G., Derewenda, Z. S. & Waugh, D. S. (2004). *Structure*, **12**, 301–306.
 Evans, G. & Pettifer, R. (2001). *J. Appl. Cryst.* **34**, 82–86.
 Evans, P. R. (1997). *Jnt CCP4/ESF–EACBM Newsl. Protein Crystallogr.* **33**, 22–24.
 Gaur, R. K., Kupper, M. B., Fischer, R. & Hoffmann, K. M. (2004). *Acta Cryst.* **D60**, 965–967.
 Harrington, A. T., Hearn, P. D., Picking, W. L., Barker, J. R., Wessel, A. & Picking, W. D. (2003). *Infect. Immun.* **71**, 1255–1264.
 Jancarik, J. & Kim, S.-H. (1991). *J. Appl. Cryst.* **24**, 409–411.
 Johnson, S., Deane, J. E. & Lea, S. M. (2005). *Curr. Opin. Struct. Biol.* **15**, 700–707.
 Leslie, A. G. W. (1992). *Jnt CCP4/ESF–EACBM Newsl. Protein Crystallogr.* **26**.
 Matthews, B. W. (1968). *J. Mol. Biol.* **33**, 491–497.
 Menard, R., Sansonetti, P. & Parsot, C. (1994). *EMBO J.* **13**, 5293–5302.
 Menard, R., Sansonetti, P. & Parsot, C. (1993). *J. Bacteriol.* **175**, 5899–5906.
 Mueller, C. A., Broz, P., Muller, S. A., Ringler, P., Erne-Brand, F., Sorg, I., Kuhn, M., Engel, A. & Cornelis, G. R. (2005). *Science*, **310**, 674–676.
 Phalipon, A. & Sansonetti, P. J. (2003). *Crit. Rev. Immunol.* **23**, 371–401.
 Picking, W. L., Nishioka, H., Hearn, P. D., Baxter, M. A., Harrington, A. T., Blocker, A. & Picking, W. D. (2005). *Infect. Immun.* **73**, 1432–1440.
 Vornrhein, C., Blanc, E., Roversi, P. & Bricogne, G. (2005). In *Crystallographic Methods*, edited by S. Doublé. Totowa, NJ, USA: Humana Press.